



Experimental investigation of the effect of Al_2O_3 nanoparticles with spherical and rod-shaped morphologies on the thermophysical properties of ionic nanofluids

S. Asleshirin^a, H. Mazaheri^{a,*}, M.R. Omidkhah Nasrin^b, and A. Hassani Joshaghani^a

a. Department of Chemical Engineering, Arak Branch, Islamic Azad University, Arak, Iran.

b. Department of Chemical Engineering, Faculty Engineering, Tarbiat Modares University, Tehran, Iran.

Received 6 May 2020; received in revised form 11 December 2020; accepted 22 February 2021

KEYWORDS

Alumina nanoparticle;
 Thermal conductivity coefficient;
 Density;
 Heat capacity;
 Ionic liquids.

Abstract. Ionic Liquids (ILs) are the fluids that are liquid at temperatures above 100°C , called “Green” solvents, and they enjoy a wide range of applications in the industry. One of their applications can be found in heat transfer and solar collectors. Thermophysical properties of liquids can be improved by adding nanoparticles to the ILs. Therefore, spherical and rod-shaped alumina nanoparticles were added to 1-Hexyl-3-methylimidazolium hexafluorophosphate ILs with different weight percentages. The effect of adding rod-shaped and spherical alumina nanoparticles on the thermophysical properties of ILs such as density, viscosity, thermal conductivity, and heat capacity to 0.05, 0.1, and 0.5% wt of nanoparticles at temperatures of 20, 30, and 50°C was investigated. Increasing the concentration of nanoparticles led to an increase in density, viscosity, and thermal conductivity and a reduction in the specific heat capacity of the Ionic Nano-Fluid (INF) compared to the base IL. Also, the viscosity, density, and thermal conductivity of INF with rod-shaped alumina nanoparticles were improved more than spherical alumina nanoparticles. Moreover, the experimental viscosity and thermal conductivity data were fitted with the existing theoretical models. The findings highlighted that the viscosities of spherical and rod-shaped alumina ILs were in unison with particles aggregation effect (Krieger-Dougherty model) and the effective thermal conductivity of INF was prognosticated by the interfacial layer approach with sufficient accuracy. Moreover, nonlinear equations were also proposed for changes in the thermophysical properties of viscosity and thermal conductivity with temperature, which showed good agreement.

© 2021 Sharif University of Technology. All rights reserved.

1. Introduction

Nanoparticles are the particles that can be measured on a nanoscale, and adding nanoparticles to base-fluids,

such as ethylene glycol, water, or oil, improves the thermophysical properties of nanofluids such as density, viscosity, and thermal conductivity [1]. A number of previously explored reasons for improving the thermal conductivity of nanofluids following the addition of nanoparticles are: 1) large specific surface area of nanoparticles for heat transfer because of its nano-sized dimension and 2) increase in the turbulence and mixing of fluid flow by displacement and mobility of

*. Corresponding author. Fax: +98 8634134023
 E-mail address: h-mazaheri@iau-arak.ac.ir (H. Mazaheri)

nano-particles, leading to the enhancement of nanofluid thermal conductivity.

ILs are organic compounds composed of ions including cations and anions. Usually, a bulky organic compound plays the role of cation; however, anions are much smaller in size than cations and have a mineral structure. Due to the difference between anion and cation parts in terms of size, the bonding of these two IL constituents is weak and they turn into liquid below 100°C. ILs enjoy a variety of applications, with the most common use as solvents, catalyst, and lubricant. These fluids can play a role in heat transfer [2]. ILs are new candidates for use in solar collectors [3–5]. Adding nanoparticles to ionic fluids is a new subject that has been recently studied by researchers [6]. By adding nanoparticles to ILs, the thermophysical properties of ionic fluids are improved, which can be very important in applying these fluids to heat transfer. Most of the research studies in this field were conducted by Nieto, and the term “Ionanofluids” was first used in 2009 by Nieto et al. [7–9].

Ribeiro et al. [10] investigated the thermal properties of ILs with and without adding nanoparticles. In their research, five ionic fluids including $[C_{6MIM}][BF_4]$, $[C_{4MIM}][PF_6]$, $[C_{6MIM}][PF_6]$, $[C_{4MIM}][CF_3SO_3]$, and $[C_{4mpyrr}][(CF_3SO_2)_2N]$ with a single-wall carbon nanotube were used. The temperature variations of 293 to 353 K and adding nanoparticles to ILs increased the thermal conductivity from 2% to 9% and increased the thermal capacity by more than 8%. Nieto et al. [11] measured two important thermodynamic properties, i.e., thermal conductivity and heat capacity, for $[C_{4MIM}][NTf_2]$ and $[C_{4MIM}][Cl]$ ionic fluids in the presence of Carbon Nano-Tubes (CNTs). They revealed that increasing the concentration of MWCNT intensified the thermal conductivity and, also, the thermal capacity slightly increased following the addition of CNTs to ILs. Having added graphene, Nieto de Castro et al. [12] investigated the thermodynamic properties, i.e., viscosity and density of ionic nanofluids at medium to high temperatures. Because conventional fluids such as water and ethylene glycol are not suitable for use at high temperatures, the mentioned researchers used ILs instead. They employed Au, Cu, CNT nanoparticles, and tetrafluoroborate ($[H_{MIM}][BF_4]$) ionic fluid. For nanofluid stabilization, ultrasonic waves alone were used. They showed that upon increasing the graphene concentration, the thermal conductivity increased and the density decreased. Franca et al. [13] studied the thermodynamic properties of two ILs, 1-ethyl-3-methyl imidazolium dicyandiamide ($[C_{2MIM}][dca]$) and 1-butyl-1-methyl pyrrolidinium cyanamide ($[C_{4mpyr}][dca]$), in the presence of CNT at temperatures ranging from 293 to 343 K. They noted that the addition of surfactant reduced the stability and

the thermal conductivity of the INFs [14]; therefore, they only used ultrasonic to prepare stable nanofluids. Furthermore, the effect of temperature on the thermal conductivity of ionic nanofluids was studied. Wang et al. [15] analyzed the effects of various parameters including temperature, dispersion conditions, size of nanoparticles, and viscosity of the base fluid on thermal conductivity and heat transfer mechanisms of INF in the presence of gold nanoparticles.

They considered the Brownian motion an effective parameter for increasing the thermal conductivity of ILs in the presence of nanoparticles and proposed the mechanisms of thermal conductivity of ILs. Elise et al. [16] utilized $[C_{4MIM}][Tf_2N]$ IL at various weight percentages of ZnO, SiO₂, CNT, and graphene nanoparticle and emphasized the enhancement of the thermal stability only through the addition of 10 wt% nanoparticles. Each nanoparticle reveals unique impact on the thermophysical behavior of nanofluid. Nanoparticle type could change the nanofluid viscosity. CNT has a diminishing effect on heat conductivity by increasing temperature; however, Al₂O₃ is treated inversely, i.e., heat conductivity enhanced by increasing temperature. The thermal conductivity of ZnO, SiO₂, and Graphene has been determined by the chemical structure and morphology of the used nanoparticle. Titan and Morshed [17] applied 1 wt% of Al₂O₃ in $[C_{4MIM}][NTf_2]$ and enhanced the thermal conductivity coefficient and heat capacity by 6% and 23%, respectively, against the pure IL. They demonstrated that ILs were good alternatives to solar collectors. Franca et al. [18] employed CNT in $[C_{2MIM}][EtSO_4]$ and $[C_{4MIM}][(CF_3SO_2)_2N]$ ILs and measured thermal conductivity at different temperatures. They demonstrated that water addition could decrease thermal conductivity. Thermal conductivity was fitted by the Nieto model in their study [19]. Finally, they concluded that CNT enhanced thermal conductivity by 6 to 26% in comparison with pure IL.

Liu et al. [20] used $H_{MIM}(BF_4)$ and nano graphene in the range of 25 to 30°C and reported that the thermal conductivity was enhanced by 15 to 22 wt% and the density and heat capacity decreased, compared to the base fluid. Therefore, they recommended this type of IL for solar collectors. Titan et al. [21] tested the hybrid N_{41111} -NTF₂ IL by carbon black and expressed that the addition of nanoparticles led to greater thermal conductivity. In addition, increase in temperature reduced the viscosity of IL quickly. Fuxian et al. [22] investigated $H_{MIM}(BF_4)$ IL with graphene nanoparticles without any surfactant at temperatures of 25 to 65°C. They noted that higher temperatures increased thermal conductivity and heat capacity and reduced viscosity, compared to the base fluid. Ferreira and Simões [23] considered four different ILs based on CNT and Phosphonium and showed that the thermal conductivity (weight percentage) was enhanced

through the addition of nanoparticles. Moreover, they studied the heat capacity and thermal stability of INF. Titan et al. [24] studied the effect of adding 0.5, 1, and 2.5 wt% of Al_2O_3 to four different ILs. They measured the viscosity, thermal conductivity, and heat capacity and highlighted their changes in comparison to base fluid. Hua Xie et al. [25] examined $\text{E}_{MIM}(\text{Dep})$ IL in the presence of CNT and water and considered the effect of temperature, different mole percentages of water, and different weight percentages of nanoparticles on the thermophysical properties of the mixture of thermal conductivity, viscosity, and density. They reported that thermal conductivity was enhanced by 1.3 to 9.7 times the base fluid and thermal conductivity was a linear function of temperature, viscosity, and density.

Most of the above papers have employed CNT and graphene nanoparticles while neglecting to investigate the effect of the shape of nanoparticles. Therefore, this paper aims to investigate the effects of the temperature and concentration as well as the shape effect of Al_2O_3 nanoparticles on the thermal conductivity, viscosity, density, and specific heat capacity of $[\text{C}_{6\text{MIM}}][\text{PF}_6]$ ILs. The experimental viscosity and thermal conductivity data were fitted with the existing theoretical models. The theoretical equations based on the mechanism of fluid layer formation around the nanoparticles were fitted with the experimental data. Finally, two nonlinear equations were consistent with the experimental data of viscosity and thermal conductivity, which showed a good fit.

2. Materials and Methods

2.1. Materials

2.1.1. Ionic liquid

In this research, IL was purchased from Research Institute of Chemistry and Chemical Engineering of Iran. This ionic liquid was given with a molecular formula of $\text{C}_{10}\text{H}_{19}\text{F}_6\text{N}_2\text{P}$ at 293 K and some of its thermophysical properties were as follows: its density 1.297 g/cm^3 , thermal conductivity 0.147 W/m.K , viscosity 789 cp , and heat capacity $1.95 \text{ J/g.}^\circ\text{C}$.

2.1.2. Al_2O_3 nanoparticles

In this study, two different nanoparticles were synthesized and then, added to the IL, as briefly described below.

2-1-2-1. Al_2O_3 spherical shape nanoparticles synthesis

Spherical nanoparticles of Al_2O_3 were synthesized and ammonium chloride (37.4 mmol) of 2.0 g was added to a 20 mL aqueous solution consisting of 1.6 g sodium salicylate. The solution was stirred for 15 min. Then, 4 mL ammonia solution (25% aqueous) was added and the mixture was stirred again for 30 min. Then, 1.33 g AlCl_3 (10 mmol) was dissolved in 5.0 g distilled

water, which was slowly added to the above solution. Its pH was adjusted to $\text{pH} = 10$ by the addition of ammonia solution and the resulting mixture was stirred for 3 h. The mixture was transferred into a stainless steel autoclave and hydrothermally treated at 393 K for 24 h. The light-yellow solid was collected through filtration, washed with water, and dried at room temperature under vacuum. Thus, spherical alumina nanoparticles with particle sizes of 30 and 50 nm were synthesized [26].

2-1-2-2. Al_2O_3 rod-shaped nanoparticle synthesis

Initially, $\text{Al}(\text{NO}_3)_3 \cdot 9\text{H}_2\text{O}$ and $(\text{NH}_4)_2\text{CO}_3$ with a molar ratio of 9:1 were mixed and solved in 100 ml water; then, the prepared solution was inserted in an autoclave with a capacity of 200 ml. The autoclave was kept in an oven for 24 h at 150°C to perform the reaction. At the end of the process and when the autoclave reached the environment temperature, the solution was poured on the filtration paper and then, washed with deionized water. Next, the produced white powder was maintained at 90°C to remove all the water content of the material. Finally, the material in a metallic holder was kept in a tubular furnace and was heated up to 450°C at a rate of 5°C/min to calcinate the nanoparticles in neutral atmospheric conditions [27].

2.2. Preparing INF and measuring its stability

In this research, INF was created through a two-step method. In other words, at first, nanoparticles were synthesized and characterized and then, were dispersed in the base fluid.

The morphology of the nanoparticles and their sizes have been characterized by the FE-SEM (Field Emission Scanning Electron Microscopy) and TEM (Transmission Electron Microscopy) method.

Rod-shaped and spherical Al_2O_3 nanoparticles were prepared through co-precipitation method. Figure 1 illustrates the FE-SEM and TEM images of the sample. According to this figure, Al_2O_3 nanoparticles were manufactured in two desired shapes (rod and spherical). The size of the spherical Al_2O_3 could be detected in the range of 30 and 50 nm. The SEM and TEM images illustrated that the synthesized nanoparticles were prepared with a uniform size domain and a specific morphology.

Nanofluid stability is one of the crucial parameters of nanofluid properties, given that semi-stable fluids precipitate very soon in the solution and cause dramatic effects, thus disrupting thermal systems and resetting INF properties to their initial state. Thus, this study employs the INF ultrasonic device for the purpose of stabilization and it is worth mentioning that INF does not need any surfactant additives for stabilization [11]. To evaluate the stability of the samples, visual analysis was first carried out by taking

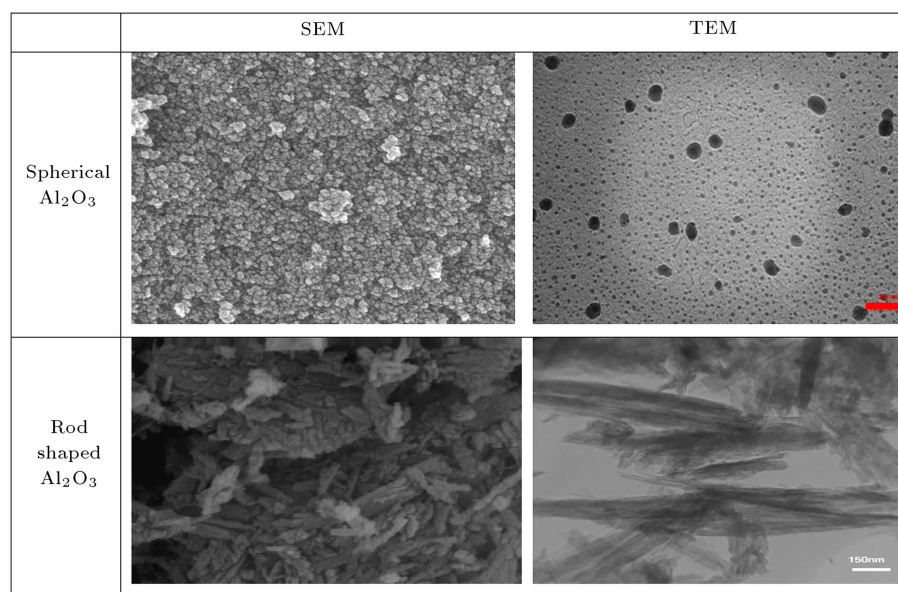


Figure 1. The SEM and TEM images of rod-shaped and spherical Al_2O_3 .

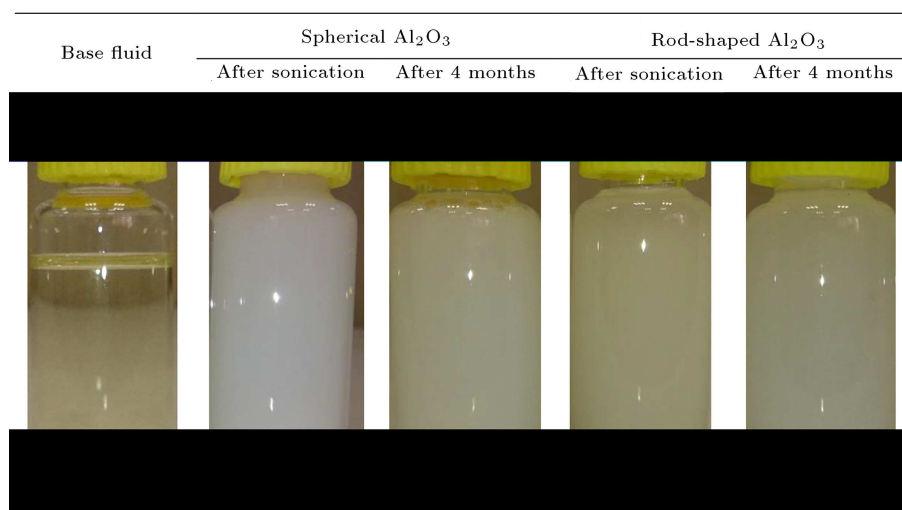


Figure 2. Visual stability analysis of the rod-shaped and spherical Al_2O_3 after four months.

photos and then, SEM and DLS protocols were applied to check the stability of rod-shaped and spherical Al_2O_3 INFs.

To investigate INFs over time, different images of the solution were taken and the color of the solutions was checked. As is evident from Figure 2, the base fluid is colorless and clear and following the addition of nanoparticles, it turns to be turbid. Figure 2 shows that the spherical Al_2O_3 nanofluids remained stable for four months without any precipitation and coagulation. Although the rod-shaped Al_2O_3 nanofluid was stable after sonication, after 4 months, some solid precipitation was detected at the bottom of the sample pot, which could be attributed to the adhesion of the particles and the formation of the solid lump. Formation of hunk bodies on the fluid surface led to the

domination of gravitational force with respect to the intermolecular force and precipitation at the bottom of the pot.

According to Figure 3, the SEM images of spherical Al_2O_3 showed a very slow formation of lump body in comparison with the rod-shaped nanoparticles. These results were confirmed based on the images presented in Figure 2 for rod-shaped Al_2O_3 .

Figure 4 depicts the particle size distribution of rod-shaped and spherical Al_2O_3 INFs after four months. According to this figure, the size of spherical Al_2O_3 ionic nanofluid does not show an impressive size change after four months. Nevertheless, the rod-shaped Al_2O_3 size experiences groundbreaking changes that verify the precipitation and coagulation of this type of Al_2O_3 nanoparticle. To sum up, the lower stability

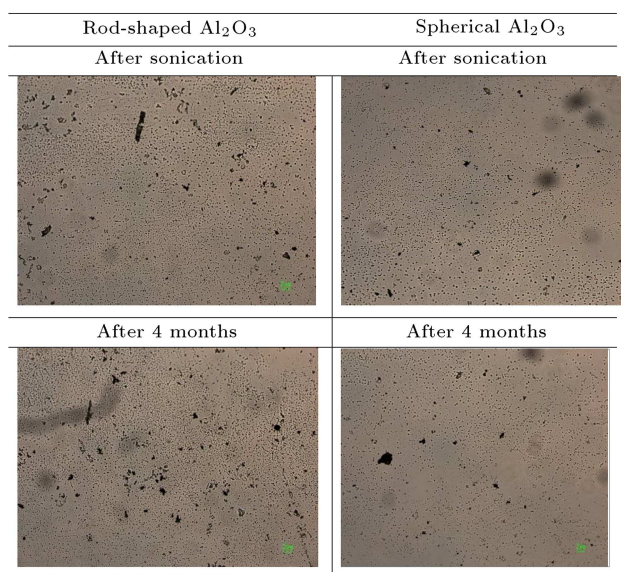


Figure 3. The SEM images of rod-shaped and spherical Al₂O₃ after four months.

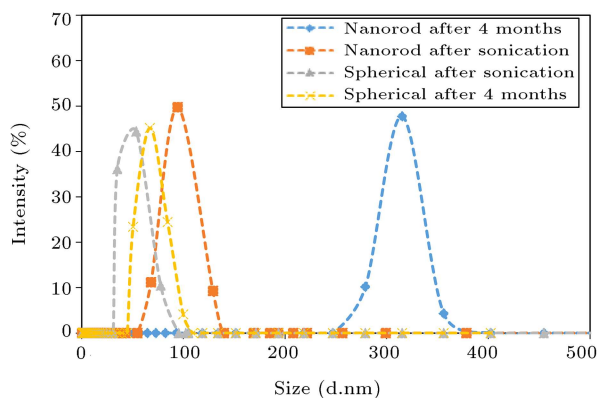


Figure 4. DLS stability analysis of the rod-shaped and spherical Al₂O₃.

of rod-shaped Al₂O₃ is attributed to the larger size of the particles on the base fluid surface.

According to the obtained stability results, the prepared ionic nanofluids have the required credibility for measuring thermophysical properties. Furthermore, the thermophysical properties of INFs including density, viscosity, thermal conductivity, and heat capacity

are compared with those of the base fluid, and the effects of temperature, nanoparticles concentration, and nanoparticles morphology (spherical and rod-shaped) on the thermal conductivity coefficient of ionic fluid are studied.

2.3. Thermophysical properties measurements

In this study, a pycnometer was used for measuring density (ASTM D153), and Ostwald viscometer, according to the ASTM D445-06, was applied to viscosity measurements. For calibration of U-shaped Ostwald viscometer, water with a factor of 0.003 was used. For removing temperature effects on the viscosity values, viscometer was kept in an oil bath whose temperature could be adjusted with a circulator.

To measure the thermal conductivity, the KD2 Pro Thermal Properties Analyzer (Labcell Ltd., UK with a probe of 6 cm length), working based on hot-wire technique, was employed with single- and double-needle sensors for measuring thermal conductivity and resistivity. A thermal bath (Haake C25) was used for controlling the temperature of the testing sample. For measuring these parameters at different temperatures, the circulator was used to make the temperatures uniform.

In addition to the viscosity and thermal conductivity, heat capacity is one of the main factors in determining the thermal efficiency and heat transfer capability of fluids. Enhancement of thermal conductivity is a necessary rule of ensuring the high efficiency of thermal equipment, but it is not a sufficient criterion. Specific heat capacity specifies the rate of heating and cooling the materials. Given that the heat capacity of matter is directly related to the atomic structure, measuring heat capacity as a function of temperature could highlight the nano-structural properties. In this study, specific heat capacity of nanofluids was measured by the calibrated differential scanning calorimeter (DSC-111, Setaram, France). By DSC, heat flow was measured for all the fluids from the ambient temperature to 90°C with a heating rate of 10°C/min. The results of uncertainty in determining thermal conductivity, density, viscosity, and heat capacity, calculated as a mean standard error, are shown in Table 1.

Table 1. Maximum uncertainty in experimental parameters and measurement devices.

Parameters	Type	Uncertainty (%)
Temperature (T)	K type Thermocouple	±2.2
Density (ρ)	Pycnometer	±0.2
Viscosity (μ)	Brookfield digital viscometer	±1
Thermal conductivity (K)	KD2-Pro	±5
Heat capacity (Cp)	DSC	±2

3. Results and discussion

3.1. Density measurement

The effects of nanoparticle weight percentage and fluid temperature were investigated for density measurements of INF. According to the density definition (mass per volume of matter), the nanoparticle density increased regardless of the nanoparticle type. All in all, the presence of solid particles in fluid led to the density enhancement, resulting from the mass addition as a result of nanoparticle presence with minor changes in solution volume. One of the most important reasons for density enhancement may be attributed to the diminished nominal volume change of solution due to its trapping in nanoparticle clusters. Figure 5 shows the spherical Al_2O_3 INF density versus nanoparticles concentration and temperature. According to Figure 6, upon increasing temperature, density decreased because the intermolecular force was reduced and the Brownian motion of particles was enhanced at higher temperatures, which led to density abatement. The density changes for rod-shaped Al_2O_3 were more sensible than those for spherical Al_2O_3 . For example, the density of the base fluid at 30°C increased from 1.3 g/cm^3 to 1.42 g/cm^3 and 1.46 g/cm^3 for 0.1 wt% of spherical and rod-shaped Al_2O_3 , respectively. Furthermore, as it is clear, the density change for rod-shaped Al_2O_3 is more significant than that for the

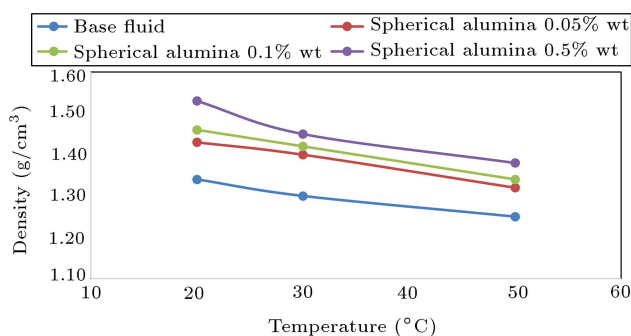


Figure 5. Density variation for the spherical Al_2O_3 ionic fluid versus nanoparticle concentration and temperature.

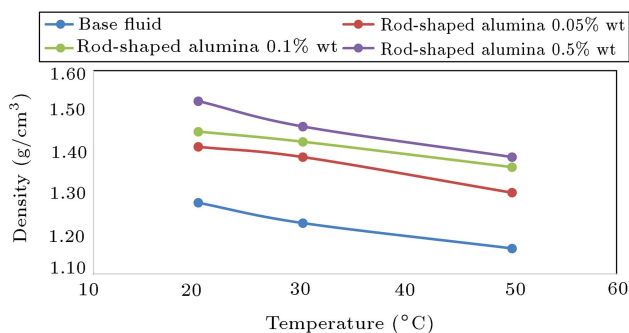


Figure 6. Density variation for the rod-shaped Al_2O_3 ionic fluid versus nanoparticle concentration and temperature.

spherical type versus concentration of nanoparticle, which is due to bulk density variation of INF and the difference in the structure of the two types of Al_2O_3 nanoparticles.

According to all the graphs, changes in the density of the INF and those in nanoparticle concentration had similar trends. Thus, as the concentration of nanoparticles increased, the density of all the investigated nanofluids was enhanced, although the density improvement was primarily connected to the intrinsic nature of the used particle. Utterly, according to the smaller increment in the density of the nanofluids than that of the base fluid, it could be inferred that density changes could not be a limiting factor in INF use.

3.2. Viscosity measurement

Viscosity is one of the key factors in the nanofluids applications, as increasing the viscosity diminishes the efficiency and increases the pump duties of the systems. For this reason, the present study explored the INF viscosity at different temperatures and concentrations of particles.

The used viscometer of this study was the U-shaped Oswald viscometer. Since the fluid viscosity was highly temperature dependent, to minimize measurement error, the viscometer should be placed in hot water bath for 20 minutes until the temperature would become constant; needless to say, each of experiment runs was repeated three times and the final values were reported as averaged values.

Generally, as mentioned before, the viscosity of nanofluids was mainly dependent on various parameters including base fluid viscosity, nanoparticle concentration, nanoparticles' shape and size, nanomaterial surface ratio, temperature, and nanoparticle aggregation tendency. Hence, the current research examined the viscosity changes for the nanoparticles including spherical and rod-shaped alumina nanoparticles against temperature and nanoparticle concentration.

Figures 7 and 8 depict variations in the ionic nanofluid viscosity of spherical and rod-shaped alumina nanofluids against temperature and nanoparticle

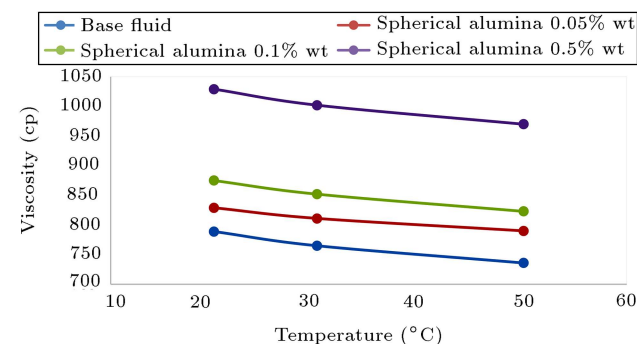


Figure 7. Viscosity changes for spherical Al_2O_3 ionic fluid versus nanoparticle concentration and temperature.

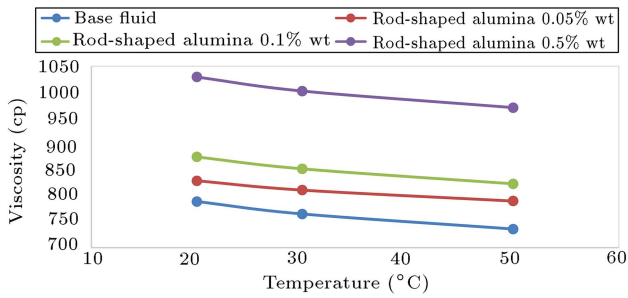


Figure 8. Viscosity changes for rod-shaped Al₂O₃ ionic fluid versus nanoparticle concentration and temperature.

concentration. According to all the measurements, increase in temperature decreased the viscosity. According to the previous discussion, the addition of concentration boosted the particle random motion and curtailed the intermolecular forces which ultimately raised the fluid flow tendency; in other words, viscosity decreased upon increase in temperature. Increasing the weight percentage of nanoparticles has ensured an increase in the viscosity of both spherical and rod-shaped alumina ionic nanofluids.

It should be noted that the nanoparticles are solid in their physical state, differing from the physical nature of the base fluid; therefore, the presence of a very small number of solid particles in the base fluid makes the fluid layers more resistant to flow. The nanoparticles have a leaning to form interconnected lattice (due to van der Waals forces between the particles) on the fluid surface, resulting in fluid viscosity variations. Based on the comparison between the obtained results of the ionic nanofluid viscosities of spherical and rod-shaped alumina nanoparticles, the viscosity of ionic base fluid increases more than the spherical alumina nanoparticles do.

For example, at 30°C, the viscosity of the base nanofluid was 765 cp, which increased following the addition of 0.1 wt% spherical and rod-shaped alumina nanoparticles to 826 cp and 852 cp, respectively. The difference in the ionic fluid viscosity of spherical and rod-shaped alumina nanofluids results from the differences in their structural shape as the rod structures escalate the tension between the fluid layers relative to the spherical structure; in addition, the base fluid is less prone to flow.

In the following, the experimental results of viscosity increment are assimilated with several common theoretical routines considering the concentration of nanoparticles.

Einstein's model [28] was deliberated as the foremost calculating viscosity model of INF at low fractions of spherical nanoparticles (< 0.02).

$$\frac{\mu_{Ionanofluid}}{\mu_{Ionicliquid}} = (1 + 2.5\phi). \quad (1)$$

Likewise, Einstein's model was modified by Brinkman

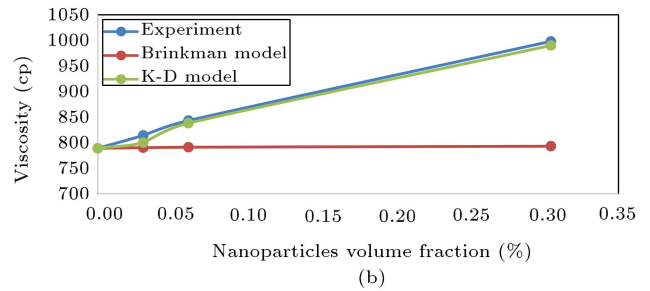
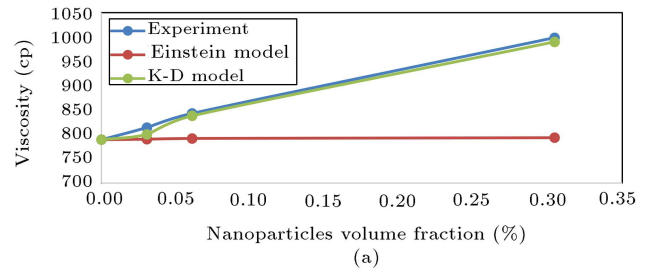


Figure 9. Variation of experimental and theoretical (a) spherical alumina IL and (b) rod-shape alumina IL viscosity as a function of particles volume fraction at 20°C.

at high concentrations of nanoparticles [29].

$$\frac{\mu_{Ionanofluid}}{\mu_{Ionicliquid}} = \frac{1}{(1 - \phi)^{2.5}}. \quad (2)$$

Likewise, involving the effects of maximum packing fraction and variable packing fractions, Krieger-Dougherty [30] managed to develop a nanofluid viscosity model.

$$\frac{\mu_{Ionanofluid}}{\mu_{Ionicliquid}} = \left(1 - \frac{\phi_a}{0.605} \left(\frac{a_a}{a}\right)^{1.2}\right)^{-1.5125}. \quad (3)$$

This formula refers to the effective volume fraction of aggregates, as presented in Eq. (4). In addition, a_a and a are the average radii of the aggregates and primary nanoparticles, respectively, and D denotes the fractal index whose typical value is 1.8 for nanofluids.

$$\phi_a = \phi \left(\frac{a_a}{a}\right)^{3-D}. \quad (4)$$

According to Figure 9, the experimental viscosity of both INFs (spherical and rod-shaped alumina) was fitted with Krieger-Dougherty (K-D) model at the aggregation factor of $aa/a = 16 - 18$. As the Krieger-Dougherty (K-D) model predicted, the nanoparticles exhibited a great tendency for aggregation; on account of this affinity, the INF viscosity increased, but other parameters like IL interplays and the surface area of nanoparticles should be regarded as hyper-efficient factors to precisely predict INF viscosity.

Table 2 shows the equation corresponding to the viscosity diagram in terms of temperature for the two spherical nanoparticles and the alumina rod in IL at a weight percentage of 0.5%.

Table 2. Viscosity equation in terms of temperature for two spherical and rod alumina nanoparticles in IL.

Nano particle	Equation
Spherical alumina 0.5%wt	$0.085T^2(^{\circ}C)-7.7T(^{\circ}C)+1118.5=\mu(cp)$ $R^2 = 1$
Rod-shaped alumina 0.5%wt	$0.0367T^2(^{\circ}C)-4.533T(^{\circ}C)+1105=\mu(cp)$ $R^2 = 1$

3.3. Thermal conductivity coefficient

As mentioned earlier, the KD2 Pro device was employed to measure the heat transfer coefficient of the nanofluids. The sample was poured into the glass container and the sensor was inserted into the pot such that the sensor was held precisely perpendicular, in which no collision with the container wall occurred. Then, the glass container was added to the ethylene glycol bath and the bath temperature was adjusted using a circulator. To set the temperature, the sample was allowed to stay for 15 minutes in the bath until a steady state could be maintained. Measurements were repeated three times for each sample at each temperature. The thermal conductivity of each sample was measured at concentrations of 0.05, 0.1, and 0.5 wt% and temperatures of 20, 30, and 50°C, respectively.

In the following, we will argue the obtained results of different nanofluids. Thermal conductivity coefficients of spherical and rod-shaped alumina ionic nanofluids were probed by changing the concentration of nanoparticles and the fluid temperature. In Figures 10 and 11, the thermal conductivity coefficients of both formulated fluids can be seen in relation to the base fluid. As can be seen, temperature and concentration had a significant impact on the thermal conductivity improvement of the base fluid, in which the temperature changes of 20°C to 50°C stimulated a relative change in the nonlinear thermal conductivity. Moreover, the changes in the thermal conductivity coefficient versus the nanoparticle concentration do not behave linearly. Based on a comparison between the results, the improvement rate of thermal conductivity of ionic nanofluids containing spherical

alumina nanoparticles was superior to that of rod-shaped alumina.

For example, at 50°C for 0.1 wt% of nanoparticles, the thermal conductivity rates of spherical alumina ionic nanofluid and rod-shaped alumina ionic nanofluid were $0.176 \text{ Wm}^{-1}\text{K}^{-1}$ and $171 \text{ Wm}^{-1}\text{K}^{-1}$, respectively. Upon increase in the concentration to 0.5 wt%, thermal conductivity rates increased to $0.189 \text{ Wm}^{-1}\text{K}^{-1}$ and $0.178 \text{ Wm}^{-1}\text{K}^{-1}$. As is clear, although spherical alumina ionic fluid had higher thermal conductivity at all measured concentrations and temperatures, the growth rate of thermal conductivity against concentration change for rod-shaped ionic nanofluid was more effective than spherical alumina ionic nanofluid. In other words, the concentration changes affect thermal conductivity more thoroughly in ionic rod-shaped alumina nanofluids. In general, as formerly stated, increasing the concentration of nanoparticles generates an interconnected network of nanoparticles on the base fluid surface and serves as thermal bridges among the base fluid surfaces.

In order to examine the mechanism of heat transfer improvement in spherical and rod-shaped alumina INFs more meticulously, the experimental thermal conductivity of these nanofluids was correlated with the estimated values using theoretical models, two of the most important relations of which are the Maxwell [31] and Hamilton equations [32]. These two models are presented in Eqs. (5) and (6):

Maxwell equation:

$$k_{eff} = \frac{k_P + 2k_f + 2(k_P - k_f)\phi}{k_P + 2k_f - 2(k_P - k_f)\phi} k_f, \quad (5)$$

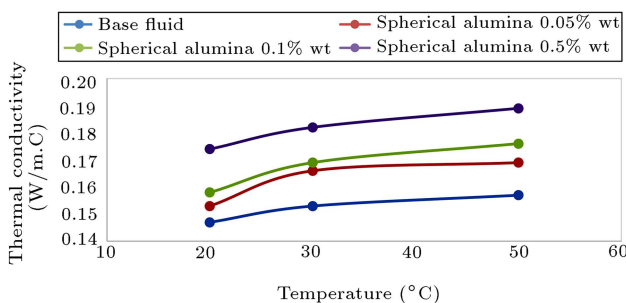


Figure 10. Thermal conductivity variations for spherical Al_2O_3 -IL versus nanoparticle concentration and temperature.

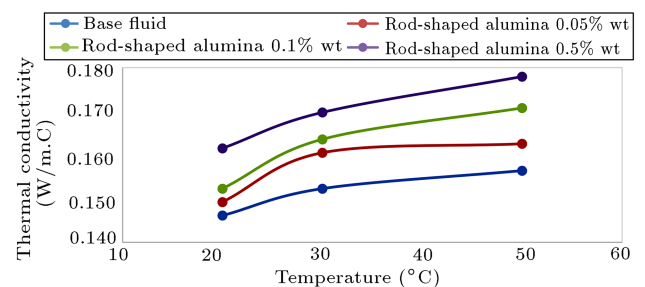


Figure 11. Thermal conductivity variations for rod-shaped Al_2O_3 -IL versus nanoparticle concentration and temperature.

Table 3. Thermal conductivity equation in terms of temperature for two spherical and rod alumina nanoparticles.

Nano particle	Equation
Spherical alumina 0.5%wt	$K(\text{W/m}\cdot^\circ\text{C}) = -0.00002T^2(^\circ\text{C}) + 0.0016T(^\circ\text{C}) + 0.149$ $R^2 = 1$
Rod-shaped alumina 0.5%wt	$K(\text{W/m}\cdot^\circ\text{C}) = 0.000001T^2(^\circ\text{C}) + 0.0015T(^\circ\text{C}) + 0.138$ $R^2 = 1$

where k_f is the thermal conductivity of the base fluid, k_P is the thermal conductivity of the solid particles, k_{eff} is the thermal conductivity of the nanofluid, and ϕ denotes the volume fraction of the solid particles in the mixture.

Hamilton equation:

$$k_{eff} = \frac{k_P + (n - 1)k_f - (n - 1)\phi(k_f - k_P)}{k_P + (n - 1)k_f + \phi(k_f - k_P)} k_f, \quad (6)$$

$$n = \frac{3}{\psi}, \quad (7)$$

in which, n denotes the shape coefficient and ψ stands for sphericity. For rod-shaped alumina nanoparticle, this model predicts more accurate results as the effect of nanoparticle shape is also taken into account for the calculation of thermal conductivity.

Afterwards, having added the effects of nanoparticle interfacial layer in the base fluid, Murshed et al. [28] attempted to determine the effective thermal conductivity of nanofluids. Eq. (8) is shown in Box I, where k_{lr} is the thermal conductivity of the interfacial layer in which $k_{Bl} < k_{lr} < K_n$; where $K_{lr} = 0.35$. γ and γ_1 are evaluated through Eqs. (9) and (10) in the following:

$$\gamma = 1 + \frac{h}{a}, \quad (9)$$

$$\gamma_1 = 1 + \frac{h}{2a}, \quad (10)$$

where h is the interfacial layer thickness of $h = 2$ and $a = 15$ nm. Figure 12 shows a comparison of the experimental findings of ionic nanofluidic datasets including spherical alumina particles with Maxwell model data and the results of rod-shaped nanoparticles predictions with Hamilton model and experimental data. According to Figure 12, the interfacial layer model was successful in predicting the effective thermal conductivity of both INFs with a passable error. The

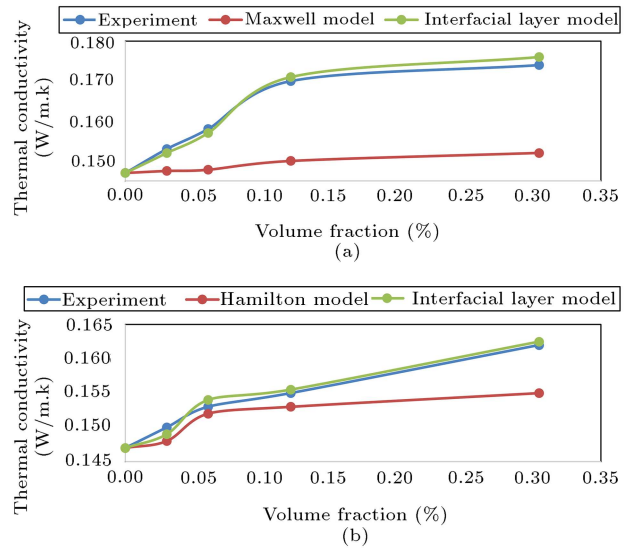


Figure 12. Variation of experimental and theoretical (a) spherical alumina IL and (b) rod-shape alumina IL thermal conductivity as a function of particles volume fraction at 20°C.

interfacial layer model predicted the experimental thermal conductivity satisfactorily with arbitrary interfacial layer thickness and thermal conductivity; however, it should be noted that other effective factors, such as interactions between nanoparticle surface and ILs, play a key role in the impeccable mechanism of increasing the thermal conductivity, which was anticipated upon the addition of nanoparticles to ILs.

The equation corresponding to the nonlinear thermal conductivity diagram in terms of temperature for the weight percentage of 0.5% of spherical nanoparticles and alumina rods in ionic fluid is given in Table 3, which shows a good fit.

3.4. Effective specific heat capacity

Heat capacity can be defined as the amount of heat needed to change the temperature of 1°C per unit volume of matter, which plays a significant role in

$$K_{\text{Ionanofluids}} = \frac{(k_n - k_{lr})\phi k_{lr} [2\gamma_1^2 - \gamma^2 + 1] + (k_n + 2k_{lr})\gamma_1^2 [\phi\gamma^2 (k_{lr} - k_{Bl}) + k_{bl}]}{\gamma_1^2 (k_n + 2k_{lr}) - (k_n - k_{lr})\phi [\gamma_1^2 + \gamma^2 - 1]} \quad (8)$$

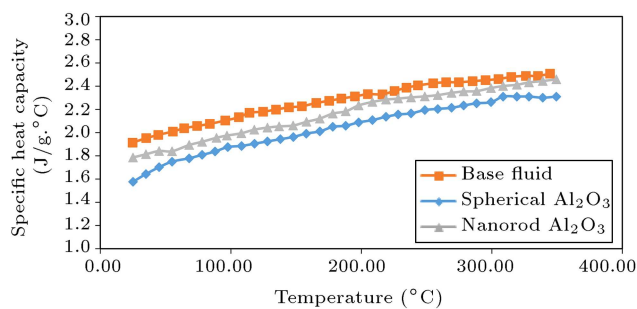


Figure 13. Heat capacity variations for rod-shaped and spherical Al₂O₃ ionic nanofluid versus temperature at 0.1 wt% of nanoparticle.

the functionality of thermal systems because it can ascertain whether the fluid in test is efficient enough to hold or transfer heat. In the present study, heat capacity variations were explored by fluctuating the temperature at 0.1 wt% of nanoparticles in the temperature range of 25 to 345 °C at an increasing rate of 10 °C.

Figure 13 illustrates the variations in the heat capacity of ionic nanofluids of spherical and rod-shaped alumina nanoparticles. As can be noticed, following a change in temperature, the heat capacity of the base fluid and the ionic nanofluids was enhanced gently. The remarkable point is the decrease in the heat capacity of spherical and rod-shaped ionic nanofluids compared to the base fluid, which may be attributed to the intrinsic nature of the particles. Physically dependent nanoparticles can gain heat more or less rapidly or be able to retain heat for a more extended period of time, which diminishes or augments the heat capacity with the addition of metallic or carbon-based nanoparticles. The addition of spherical and rod-shaped alumina nanoparticles reduced the thermal capacity of the base fluid by averagely about 12 and 5%, respectively. The results highlight that to heat the nanofluids containing spherical and rod-shaped alumina nanoparticles for one-degree Celsius enhancement, they require less heat than the base fluid.

4. Conclusion and recommendations

The effects of adding spherical and rod-shaped alumina nanoparticles to 1-hexyl-3-methyl imidazolium hexafluorophosphate IL at different concentrations of nanoparticles and temperatures were investigated, and the thermophysical properties of INFs were measured. Experimental results showed that with increase in temperature, INF density decreased; upon increasing nanoparticle concentration, INF density increased and the density changes for rod-shape Al₂O₃ were more significant than those for the spherical type versus concentration of nanoparticles.

The effect of increasing the concentration of

nanoparticles on viscosity showed that increasing the weight percentage of nanoparticles led to an increase in the viscosity of both spherical and rod-shape alumina INFs. Moreover, the experimental results of viscosity increment were assimilated with several common theoretical routines considering nanoparticles concentration. The findings highlighted that the viscosities of spherical and rod-shaped alumina ILs were in unison with particles aggregation effect (Krieger-Dougherty model). Also, the effect of increasing the temperature and concentration of nanoparticles on thermal conductivity showed that temperature and concentration had a significant role in increasing thermal conductivity; this effect on INF containing rod alumina particles was greater than nanofluids containing spherical nanoparticles. Experimental thermal conductivity data were compared with the data derived from several well-known theoretical models, the results of which pointed to good agreement between these data and the model proposed by Murshed, which was based on considering the formation of the fluid layer around the nanoparticles. Finally, high-precision nonlinear equations were proposed for thermophysical properties such as viscosity and thermal conductivity. Also, the effect of increasing temperature and adding alumina nanoparticles on the heat capacity of INFs was investigated, which showed that with the addition of alumina nanoparticles, the heat capacity of ionic nanofluid decreased; this reduction was greater for the INF containing spherical particles than that for the INF containing alumina rod particles, and increasing the temperature augmented the heat capacity of the ionic nanofluid. At the end, one of the applications of IL is heat transfer from fluids and ILs present at high temperatures. It is suggested that the effect of adding nanoparticles to ionic fluid at high temperatures on the properties of this IL to be investigated.

References

1. Eastman, J.A. and Choi, U.S. "Anomalously increased effective thermal conductivities of thylene glycol-based nano fluid containing copper nano particles", *Applied Physics Letters*, **78**, pp. 718–728 (2001).
2. Vishwas, V. and Vadekar, M. "ILs as heat transfer fluids - An assessment using industrial exchanger geometries", *Applied Thermal Engineering*, **111**(25), pp. 1581–1587 (2017).
3. Lamas, A., Brito, I., Salazar, F., et al. "Synthesis and characterization of physical, thermal and thermodynamic properties of ILs based on [C12mim] and [N444H] cations for thermal energy storage", *Journal of Molecular Liquids*, **224**, pp. 999–1007 (2016).
4. Valkenburg, M.E., Vaughn, R.L., Williams, M., et al. "Thermochemistry of IL heat-transfer fluids", *Thermochimica Acta.*, **425**, pp. 181–188 (2005).

5. Saffarian, M. and Moravej, M. “Heat transfer enhancement in a flat plate solar collector with different flow path shapes using nanofluid”, *Renewable Energy*, **146**, pp. 2316–2329 (2020).
6. Guo, Y. and Liu, G. “Solvent-free ionic silica nanofluids: Smart lubrication materials exhibiting remarkable responsiveness to weak electrical stimuli”, *Chemical Engineering Journal*, **383**, pp. 123–202 (2020).
7. Ribeiro, A.P.C., Lourenço, M.J.V., and Nieto de Castro, C.A. “Thermal conductivity of ionanofluids”, *7th Symp. Thermophysical Properties*, Boulder, pp. 21–26 (2009).
8. Nieto de Castro, C.A., Lourenço, M.J.V., and Ribeiro, A.P.C. “Thermal properties of ILs and ionanofluids of imidazolium and pyrrolidinium liquids”, *J. Chem. Eng. Data*, **55**(2), pp. 653–661 (2010).
9. Nieto de Castro, C.A., Murshed, S.M.S., and Santos, F.J.V. “Enhanced thermal conductivity and specific heat capacity of carbon nanotubes ionanofluids”, *Int. J. Therm. Sci.*, **62**, pp. 34–39 (2012).
10. Ribeiro, A.P.C., Vieira, S.I.C., and Franca, J.M. “Thermal Properties of ILs and Ionanofluids” (2010).
11. Nieto de Castro, C.A. and Murshed, S.M.S. “Enhanced thermal conductivity and specific heat capacity of carbon nanotubes ionanofluids”, *International Journal of Thermal Sciences*, **62**, pp. 34–39 (2012).
12. Nieto de Castro, C.A., Murshed, S.M.S., Lourenço, M.J.V., et al. “Enhanced thermal conductivity and specific heat capacity of carbon nanotubes ionanofluids”, *International Journal of Thermal Sciences*, **62**, pp. 34–39 (2012).
13. Franca, J.M.P., Vieira, S.I.C., Lourenço, M.J.V., et al. “Thermal conductivity of [C4mim][(CF3SO2)2N] and [C2mim][EtSO4] and their IoNanofluids with carbon nanotubes: Experiment and theory”, *Journal of Chemical & Engineering Data*, **58**(2), pp. 467–476 (2013).
14. Murshed, S.M.S., Nieto de Castro, C.A., et al. “Effect of surfactant and nanoparticle clustering on thermal conductivity of aqueous nanofluids”, *J. Nanofluids*, **1**, pp. 175–179 (2012).
15. Wang, B. and Wang, X. “IL-based stable nanofluids containing gold nanoparticles”, *Journal of Colloid and Interface Science*, **362**, pp. 5–14 (2011).
16. Elise, B.F., Ann, E.V., Nicholas, J., et al. “Thermophysical properties of Nanoparticle-Enhanced ILs (NEILs) heat-transfer fluids”, *Energy Fuel*, **16**, pp. 3385–3393 (2013).
17. Titan, C.P. and Morshed, A.K. “Nanoparticle enhanced ILs(NEILs) as working fluid for the next generation solar collector”, *Procedia Engineering*, **56**, pp. 631–636 (2013).
18. Franca, J.M.P., Reis, F., and Vieira, S.I.C. “Thermophysical properties of IL dicyanamide (DCA) nanosystems”, *J. Chem. Thermodynamics*, **79**, pp. 248–257 (2014).
19. Nieto de Castro, C.A., Lourenço, M.J.V., Ribeiro, A.P.C., et al. “Thermal Properties of ILs and IoNanofluids of Imidazolium and Pyrrolinium Liquids”, *J. Chem. Eng. Data*, **55**, pp. 653–661 (2010).
20. Liu, J., Wang, F., Zhang, L., et al. “Thermodynamic properties and thermal stability of ionic liquid-based nanofluids containing graphene as advanced heat transfer fluids for medium-to-high-temperature applications”, *Renewable Energy*, **63**, pp. 519–523 (2014).
21. Titan, C.P., Morshed, M., and Jamil, A. “Effect of nanoparticle dispersion on thermophysical properties of ionic liquids for its potential application in solar collector”, *Procedia Engineering*, **90**, pp. 643–648 (2014).
22. Wang, F., Han, J., Zhang, Z., et al. “Surfactant-free ionic liquid-based nanofluids with remarkable thermal conductivity enhancement at very low loading of graphene”, *Nanoscale Research Letters*, **7**, pp. 276–314 (2012).
23. Ferreira, A.G.M. and Simões, P.N. “Transport and thermal properties of quaternary phosphonium ionic liquids and IoNanofluids”, *J. Chem. Thermodynamics*, **64**, pp. 80–92 (2013).
24. Titan, C.P. and Murshed, A.K.M.M., et al. “Enhanced thermophysical properties of NEILs as heat transfer fluids for solar thermal application”, *Applied Thermal Engineering*, **110**, pp. 1–9 (2017).
25. Zongchang, H.X. and Zhao, Z.J. “Measurement of thermal conductivity, viscosity and density of ionic liquid[EMIM][DEP]-based nanofluids”, *Chinese Journal of Chemical Engineering*, **24**, pp. 331–338 (2016).
26. Astam, K.P., Dutta, A., and Bhaumik, A. “Self-assembled mesoporous-Al2O3 spherical nanoparticles and their efficiency for the removal of arsenic from water”, *Journal of Hazardous Materials*, **201**, pp. 170–177 (2012).
27. Chen, X.Y., Zhang, Z.J., Liang, X., et al. “Controlled hydrothermal synthesis of colloidal boehmite (-AlOOH) nanorods and nanoflakes and their conversion into -Al2O3 nanocrystals”, *Solid State Communications*, **145**, pp. 368–373 (2008).
28. Murshed, S.M.S., Leong, K.C., and Yang, C. “Investigations of thermal conductivity and viscosity of nanofluids”, *International Journal of Thermal Sciences*, **47**(5), pp. 560–568 (2008).
29. Alawi, O.A. and Sidik, N.A.C., et al. “Thermal conductivity and viscosity models of metallic oxides nanofluids”, *Int. J. Heat Mass Transfer.*, **116**, pp. 1314–1325 (2018).
30. Selvakumar, R.D. and Dhinakaran, S. “Effective viscosity of nanofluids - A modified Krieger-Dougherty

model based on particle size distribution (PSD) analysis”, *J. Mol. Liq.*, **225**, pp. 20–27 (2017).

31. Yu, W. and Choi, S.U.S. “The role of interfacial layers in the enhanced thermal conductivity of nanofluids: A renovated Maxwell model”, *J. Nanopart. Res.*, **5**(1), pp. 167–171 (2003).
32. Arul Raja, R.A. and Sunil, J. “Estimation of thermal conductivity of nanofluids using theoretical correlations”, *International Journal of Applied Engineering Research.*, **13**, pp. 7932–7936 (2018).

Biographies

Samira Asleshirin has a BS degree from Isfahan University of Technology and an MS degree from Arak University. She is currently a PhD Student in Chemical Engineering at the Islamic Azad University of Arak and a member of the Faculty of the Islamic Azad University of Boroujerd, Boroujerd, Iran.

Hossein Mazaheri holds a PhD in Chemical Engineering, is a Faculty Member, and an Assistant

Professor at the Islamic Azad University, Arak Branch. He completed his PhD in Chemical Engineering at the University of Malaysia in 2010 and is currently the Vice Chancellor of the Islamic Azad University of Arak and has published numerous articles in prestigious journals.

Mohammad Reza Omidkhah Nasrin holds a PhD in Chemical Engineering and is a Faculty Member and Professor at Tarbiat Modares University. He holds a Master’s degree from the University of Michigan in the United States and a PhD from the University of Manchester in the United Kingdom. He is currently the Director of the Iranian Institute of Chemistry and Chemical Engineering.

Ali Hassani Joshaghani holds a PhD in Chemical Engineering and is an Assistant Professor at the Islamic Azad University, Arak Branch. He completed his PhD in Chemical Engineering at Malaysia University of Science in 2015 and is currently the Vice Chancellor for Research at the Islamic Azad University, Arak Branch, Arak, Iran.